

efficiency,  $\eta_p^{\max}$ , obtained by eliminating  $\delta$  from Eq. (5) through a parameter  $K_\lambda \equiv \delta/2.303D_o$  and equating  $d\eta_p/dD_o=0$ , is given by

$$\eta_p^{\max} = [\sin^2(\tan^{-1}K_\lambda)] \times \exp[-(2/K_\lambda)\tan^{-1}K_\lambda], \quad (6)$$

for an optical density of  $(4 \cos\theta_o/2.303K_\lambda)\tan^{-1}K_\lambda$ . The parameter  $K_\lambda$  is found to be zero at the  $M$  peak but increases continuously along each absorption edge with typical values of 1.02, 3.03, and 4.91 rad/ $D_o$  at 485, 475, and 470 nm, respectively.<sup>11</sup> The corresponding  $\eta_p^{\max}$  would be 0.05, 0.36, and 0.53,<sup>12</sup> which are quite large particularly when compared to the absorptive contribution which is at most 0.037.<sup>1</sup>

The author is especially indebted to Matt Lehmann for the use of his laboratory facilities during the course of the investigation and for many stimulating and enlightening discussions. The author is also grateful to T. W. Hänsch for very useful suggestions and to F. C. Brown for his many informative comments and critical reading of the manuscript.

<sup>1</sup>H. Kogelnik, Bell Syst. Tech. J. **48**, 2909 (1969).

<sup>2</sup>M. Lehmann, J. Opt. Soc. Amer. **63**, 505 (1973). Dispersion effects were also indicated earlier for  $F$ -center gratings by G. E. Scrivener and M. R. Tubbs, Opt. Commun. **6**, 242 (1972).

<sup>3</sup>See F. Lüty and J. Mort, Phys. Rev. Lett. **12**, 45 (1964); J. Mort, F. Lüty, and F. C. Brown, Phys. Rev.

**137**, A566 (1965); F. C. Brown, B. C. Cavenett, and W. Hayes, Proc. Roy. Soc., Ser. A **300**, 78 (1967); H. Paus and F. Lüty, Phys. Rev. Lett. **20**, 57 (1968).

<sup>4</sup>For a general review of the anisotropic properties of  $M$  centers, see W. D. Compton and H. Rabin, in *Solid State Physics*, edited by F. Seitz and D. Turnbull (Academic, New York, 1964), Vol. 16.

<sup>5</sup>See, for example, M. Born and E. Wolf, *Principles of Optics* (Pergamon, Oxford, 1970), Sect. 1.4.2.

<sup>6</sup>An alternative, simple expression,

$$n_{\parallel} - n_{\perp} = \frac{\lambda}{2\pi a} \cos^{-1} \left( \frac{a_{\perp}^2 - a_{\parallel}^2}{2a_{\parallel}a_{\perp}} \tan 2\theta \right),$$

obtained by setting the derivative  $\partial I_{\parallel}/\partial\theta$  or  $\partial I_{\perp}/\partial\theta$  equal to zero, is also useful but apparently less accurate in very low-absorption regions.

<sup>7</sup>The sign change was determined separately using a solleil compensator.

<sup>8</sup>Assuming an oscillator strength of 0.30, this would correspond to an  $M$ -center concentration range of  $7.8 \times 10^{15}$  to  $1.1 \times 10^{18}$  cm<sup>-3</sup>.

<sup>9</sup>See M. Garbuny, *Optical Physics* (Academic, New York, 1965), Sect. 5.2.2.

<sup>10</sup>For cases of incomplete alignment or overlapping absorptions in the  $M$ -spectral region, the variable  $D_o$  in the exponential of Eq. (5) could be replaced by  $D_o/p$ , where  $p \equiv (D_{o\parallel} - D_{o\perp})/(D_{o\parallel} + D_{o\perp})$  is an effective degree of  $M$ -center alignment.

<sup>11</sup>A more detailed account of the diffraction will be presented in a later paper.

<sup>12</sup>Since moderately large dichroic  $M$  bands are needed to fully attain these efficiencies, the  $M$ -center orientation should be almost complete and it is especially important that the  $M$ -band spectral region be reasonably free of extraneous overlapping absorptions.

## Electronic-Energy-Level Measurements of Chemisorbed Oxygen on the (100) Plane of Nickel by Electron Energy-Loss Spectroscopy\*

S. Ohtani,† K. Terada, and Y. Murata

*Department of Chemistry, Gakushuin University, Mejiro, Toshima-ku, Tokyo, Japan*

(Received 16 November 1973)

Energy-loss spectra of low-energy electrons reflected from the nickel (100) plane were measured as a function of coverage by oxygen. A characteristic energy loss at 5.8 eV was observed in the  $p(2 \times 2)$  arrangement. This loss peak splits into 5.4 and 6.4 eV in  $c(2 \times 2)$ . These peaks are caused by excitation of electrons in chemisorption bonds of nickel-oxygen. The split shows the change in bond nature in the different coverages of oxygen on Ni(100).

In recent years, electronic energy levels of chemisorption bonds on metal surfaces have been measured by the use of energy analysis of electrons, that is, ion-neutralization spectroscopy (INS),<sup>1</sup> ultraviolet photoemission spectroscopy,<sup>2</sup> field-emission energy distributions,<sup>3</sup> and elec-

tron energy-loss spectroscopy.<sup>4,5</sup> Vibrational energies have also been measured by electron energy-loss spectroscopy.<sup>6,7</sup> In the present paper we wish to report on the electronic energy levels associated with chemisorbed oxygen on the nickel (100) surface measured by energy-loss

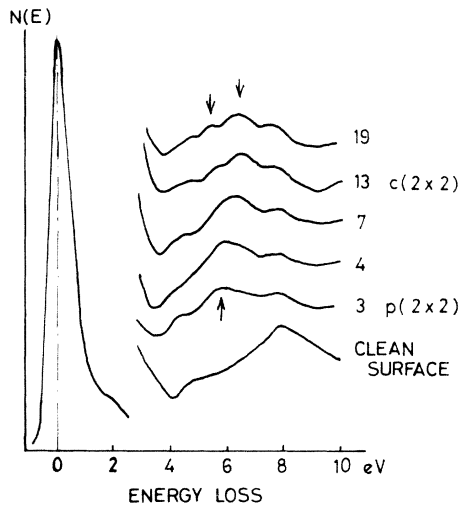


FIG. 1. Energy-loss spectra of 100-eV primary electrons reflected from a Ni(100) plane. Oxygen exposure in units of Langmuirs ( $1 \text{ L} = 1 \times 10^{-6} \text{ Torr sec}$ ). Energy-loss peaks associated with the chemisorption bond of Ni-O are shown by arrows. LEED patterns corresponding to these spectra are indicated by  $p(2 \times 2)$  and  $c(2 \times 2)$ . The ordinate represents distribution of electron energy.

spectra of low-energy electrons.

Energy-loss spectra were measured by use of a retarding-field analyzer with an energy resolution of  $\Delta E/E < 0.4\%$ . A single crystal was oriented, cut within  $1^\circ$  to the (100) face, mechanically polished, and etched in a saturated solution of iron (III) chloride at  $50^\circ\text{C}$ . It was further electropolished in 60% sulfuric acid with a current density of  $2 \text{ A/cm}^2$ . The crystal surface was cleaned by heating it to about  $800^\circ\text{C}$  in  $5 \times 10^{-10} \text{ Torr}$  for 4 h, repeating oxidation in the oxygen atmosphere of  $1 \times 10^{-6} \text{ Torr}$  at  $700^\circ\text{C}$  and reduction in the hydrogen atmosphere of  $5 \times 10^{-6} \text{ Torr}$  at  $700^\circ\text{C}$  for several hours, and finally heating to about  $900^\circ\text{C}$  for 30 min. Auger-electron spectra and low-energy electron diffraction (LEED) patterns were used to confirm the cleanliness of the crystal surface.

The nickel crystal surface was exposed to oxygen at  $1 \times 10^{-8} \text{ Torr}$  at room temperature. Energy-loss spectra of 100-eV primary electrons reflected from the nickel (100) plane are shown in Fig. 1 with various exposures to oxygen. These spectra were measured with the ac perturbation applied to the retarding grids of 1 kHz and 20 mV rms, and the corresponding 1-kHz component in the output was detected with a lock-in amplifier. In a small energy-loss region, energy-loss peaks of 1.8, 4.3, and 8.0 eV were observed in all the

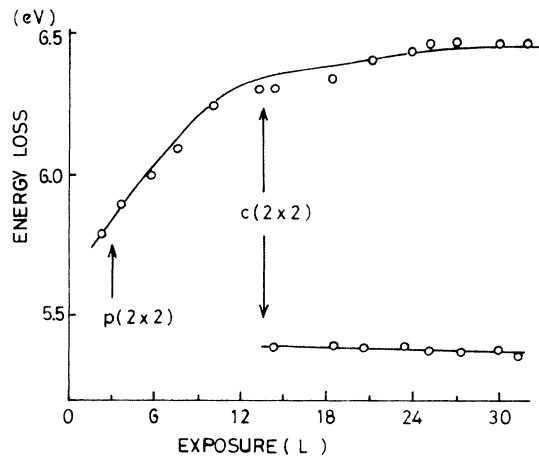


FIG. 2. Oxygen-exposure dependence of energy-loss values at about 6 eV.

oxygen coverages studied. These peak values can be assigned to the transition between the bands near the  $W$  and  $K$  symmetry points, the transition from the  $L_2'$  to the upper  $L_1$  state,<sup>8</sup> and surface plasmon excitation, respectively, and are consistent with the results obtained for the clean surface of the Ni(111) plane.<sup>9</sup>

Another loss peak of 5.8 eV, which was not detected in clean Ni(100) and Ni(111) surfaces, was observed in the  $p(2 \times 2)$  surface arrangement, that is,  $\frac{1}{4}$ -monolayer coverage. This peak shifted to a larger loss value when the adsorbed oxygen was increased, and finally split into two peaks at 5.4 and 6.4 eV in the  $c(2 \times 2)$  pattern, that is,  $\frac{1}{2}$ -monolayer coverage. The positions and the features of the split peaks were reproducible in several repeated runs of the whole experiments. The observed loss values are shown in Fig. 1, and their variations for various exposures are plotted in Fig. 2. LEED patterns in the stages between  $l(2 \times 2)$  and  $c(2 \times 2)$  showed superstructures and streaks. Auger-electron spectra were also measured at the same adsorbing conditions by the use of 1500-eV primary electrons.

Peak heights of the  $KLL$  oxygen peak<sup>10</sup> at 510 eV relative to the  $LMM$  nickel peak at 840 eV are plotted in Fig. 3. Since the shift in the loss peak shown in Fig. 2 corresponds to the amount of adsorbed oxygen shown in Fig. 3, it can be concluded that the origin of these loss peaks is the effect of oxygen, and probably the electronic excitation in chemisorption bonds of nickel-oxygen. It might be thought that these loss peaks were due to adsorption of carbon monoxide, which is a main portion of the residual gases before in-

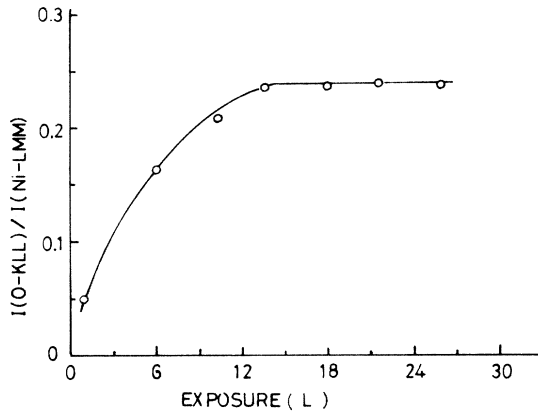


FIG. 3. Oxygen-exposure dependence of peak heights of the Auger spectra of the *KLL* oxygen peak at 510 eV relative to the *LMM* nickel peak at 840 eV.  $I(O-KLL)$  in the ordinate denotes the peak-to-peak height of a derivative of the distribution of electron energy of the *KLL* oxygen peak.

roducing oxygen, on the crystal surface. However, a small *KLL* carbon peak at 270 eV was scarcely increased in height during these measurements. Furthermore, the intensity profiles of these spectra did not change essentially for primary-electron energies of 90 to 150 eV. Therefore, the shift and splitting of the peaks observed at about 6 eV are caused by a change in bond nature in different coverages of oxygen on the Ni(100) plane instead of other origins, say, a diffraction effect. The shift in this energy-loss peak from the  $\frac{1}{4}$ - to the  $\frac{1}{2}$ -monolayer coverages may be due to the overlapping of the peaks at 5.8 eV corresponding to the  $\frac{1}{4}$ -monolayer coverage and those at 5.4 and 6.4 eV corresponding to the  $\frac{1}{2}$ -monolayer coverage in different intensities.

The change in the bond nature in the  $\frac{1}{4}$ - and  $\frac{1}{2}$ -monolayer coverages described above is further supported by observations of the changes in the work function and the characteristic energy-loss values due to core-electron excitation of Ni 3*p* at 65 eV, shown in Figs. 4 and 5, respectively. The work-function changes were determined by observing the potential shifts in the retarding-potential characteristic between the retarding grids and the sample with primary electrons of 10 or 20 eV.<sup>11</sup> Both the work function and this energy-loss value have a maximum value near the  $p(2 \times 2)$  arrangement and decrease gradually with increasing coverage. The energy-loss value due to core-electron excitation is equivalent to the binding energy of the core electron below the Fermi level and is not affected by the work-function change.

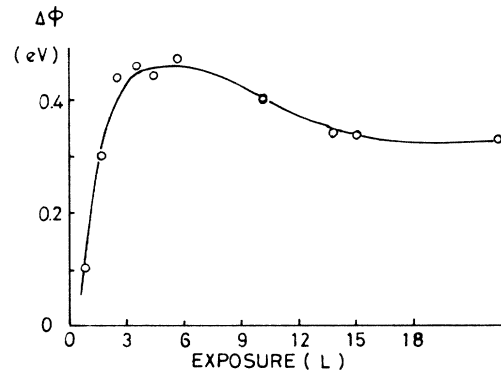


FIG. 4. Work-function change versus oxygen exposure.

If the bond nature in the  $\frac{1}{2}$ -monolayer coverage were the same as that in the  $\frac{1}{4}$ -monolayer coverage, the changes in the work function and the energy-loss value in the  $\frac{1}{2}$ -monolayer coverage might have been about twice as large as that in the  $\frac{1}{4}$ -monolayer coverage. Since the observed changes are to the contrary, one is led to the conclusion that the ionicity of oxygen atoms decreases and the covalency increases in the  $\frac{1}{2}$ -monolayer coverage.

The splitting in the  $\frac{1}{2}$ -monolayer coverage is interpreted on the basis of the following model. The oxygen atoms sit in the hollows surrounded by four nickel atoms on the surface<sup>12</sup> and have divalent bonds as derived from the above-mentioned changes in the work function and the core-excitation loss. Two kinds of interactions between the nearest-neighbor oxygen atoms, a stronger interaction through the covalent O-Ni-O bonds and a weaker one through those not linked by covalent bonds, are randomly distributed among the oxygen atoms on the surface. The for-

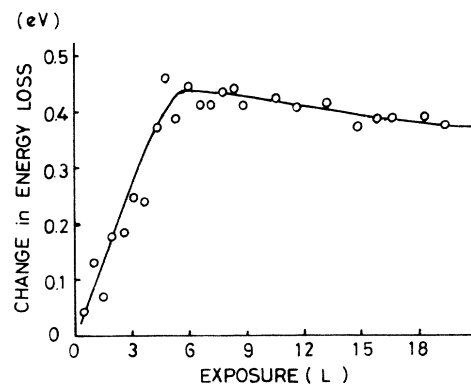


FIG. 5. Energy-loss value versus oxygen exposure for the core-electron excitation of Ni 3*p* at 65 eV.

mer interaction is similar to the superexchange in magnetic materials. The occupied energy levels of chemisorption bonds in the  $\frac{1}{2}$ -monolayer coverage split into the levels separated by a few times the interaction energy of the superexchange type. Details of the present discussion of the bond nature will be presented elsewhere.

Previous results obtained by INS<sup>1</sup> and photoemission spectroscopy<sup>2</sup> for chemisorbed oxygen on nickel surface did not show the splitting in the  $\frac{1}{2}$ -monolayer coverage, though the mean energy-loss value of about 6 eV obtained in the present observation is in agreement with either of the previous results. Küppers<sup>5</sup> also observed an energy-loss peak near 6 eV after adsorption of oxygen on the Ni(110) surface but did not observe the splitting. Since the split peaks observed in the present study are believed to be real ones, we consider the origin of this discrepancy as follows:

The photoemission results contain the effects of planes other than (100), because a polycrystalline nickel film was used. As mentioned above, the splitting observed in the  $\frac{1}{2}$ -monolayer coverage is caused by two interactions randomly distributed among the nearest-neighbor oxygen atoms. Since the above situation is not expected for the (110) plane, it is not surprising if no splitting is observed in the energy-loss spectra on Ni(110). As for the difference between the INS and the present results, no clear-cut explanation can be presented. Nevertheless, the difference might originate from differences in the treatment of the samples or in the local state density on the surface, which can depend on the method of measurement. A more detailed investigation of this problem is left for a future experiment.

The changes in the bond nature in the different coverages described above have also been observed in two previous experiments. Hagstrum and Becker<sup>1</sup> have proposed from their INS results for S and Se on Ni(100) a  $M_2X$  bridge structure in the  $c(2 \times 2)$  structure and a  $M_4X$  pyramidal

structure in the  $p(2 \times 2)$  structure. Our models for O on Ni(100) are similar to these structures. In another study<sup>3</sup> the field-emission energy distribution for the hydrogen atom adsorbed on the W(100) plane showed a change in the enhancement factor with coverages, that is, the energy distribution characteristic of  $\beta_2$  gradually shifts and converts to that characteristic of  $\beta_1$ .

The authors thank Professor K. Kuchitsu of the University of Tokyo for his discussions.

---

\*Work supported by a grant-in-aid from the Ministry of Education.

†Present address: Institute of Plasma Physics, Nagoya University, Chikusa-ku, Nagoya, Japan.

<sup>1</sup>H. D. Hagstrum and G. E. Becker, Phys. Rev. Lett. **22**, 1054 (1969), and J. Chem. Phys. **54**, 1015 (1971); G. E. Becker and H. D. Hagstrum, Surface Sci. **30**, 505 (1972).

<sup>2</sup>D. E. Eastman and J. K. Cashion, Phys. Rev. Lett. **27**, 1529 (1971).

<sup>3</sup>E. W. Plummer and A. E. Bell, J. Vac. Sci. Technol. **9**, 583 (1972).

<sup>4</sup>F. Steinrisser and E. N. Sickafus, Phys. Rev. Lett. **27**, 992 (1971).

<sup>5</sup>J. Küppers, Surface Sci. **36**, 53 (1973).

<sup>6</sup>F. M. Propst and T. C. Piper, J. Vac. Sci. Technol. **4**, 53 (1967).

<sup>7</sup>H. Ibach, Phys. Rev. Lett. **27**, 253 (1971).

<sup>8</sup>M. Shiga and G. P. Pells, J. Phys. C: Proc. Phys. Soc., London **2**, 1847 (1969).

<sup>9</sup>B. Heimann and J. Hölzl, Phys. Rev. Lett. **26**, 1573 (1971).

<sup>10</sup>The notation of the *KLL* oxygen peak is used in Auger-electron spectroscopy. See for example C. C. Chang, Surface Sci. **25**, 53 (1971).

<sup>11</sup>The present data for the work-function change do not agree with those studied by Hagstrum and Becker, who reported that the change was slightly larger for  $c(2 \times 2)$  than for  $p(2 \times 2)$ . We have no clear-cut explanation for this discrepancy, but it does not essentially influence the following discussion.

<sup>12</sup>S. Anderson, B. Kasemo, J. B. Pendry, and M. A. Van Hove, Phys. Rev. Lett. **31**, 595 (1973).